Experimental characterization of fatigue damage in a nickel-base superalloy using nonlinear ultrasonic waves

Jin-Yeon Kim, Laurence J. Jacobs,[a] and Jianmin Qu
G. W. Woodruff School of Mechanical Engineering, Georgia Institute of Technology, Atlanta, Georgia 30332-0405

Jerrol W. Littles
Pratt & Whitney, Materials and Processes Engineering, 400 Main Street, M/S 114-40, East Hartford, Connecticut 06108

(Received 10 February 2006; revised 14 June 2006; accepted 16 June 2006)

This research develops a robust experimental procedure to track the evolution of fatigue damage in a nickel-base superalloy with the acoustic nonlinearity parameter, β, and demonstrates its effectiveness by making repeatable measurements of β in multiple specimens, subjected to both high- and low-cycle fatigue. The measurement procedure developed in this research is robust in that it is based on conventional piezoelectric contact transducers, which are readily available off the shelf, and it offers the potential for field applications. In addition, the measurement procedure enables the user to isolate sample nonlinearity from measurement system nonlinearity. The experimental results show that there is a significant increase in β linked to the high plasticity of low-cycle fatigue, and illustrate how these nonlinear ultrasonic measurements quantitatively characterize the damage state of a specimen in the early stages of fatigue. The high-cycle fatigue results are less definitive (the increase in β is not as substantial) due to increased uncertainties involved in the high-cycle fatigue tests, but still show a clear relationship between β and remaining fatigue life. One application of the measured β versus fatigue-life data is to potentially serve as a master curve for life prediction based on nonlinear ultrasonic measurements. [DOI: 10.1121/1.2221557]

PACS number(s): 43.25.Zx, 43.25.Dc, 43.25.Ba [MFH] Pages: 1266–1273

I. INTRODUCTION

Recent experimental studies and new physical models are demonstrating the potential of nonlinear ultrasonics (or the second-harmonic generation technique) to quantitatively detect and characterize fatigue damage in metals.[1–10] This fatigue damage first appears in the form of dislocation substructures, such as veins and persistent slip bands (PSBs), and these PSBs accumulate at grain boundaries to produce strain localization and, then finally, microcrack initiation with increasing fatigue cycles. These dislocations (and resulting microplastic deformation) do not cause a large change in the linear macroscopic properties (such as elastic moduli, sound speed, and attenuation) of a material; the changes in the linear ultrasonic values are not large enough to be accurately measured with conventional linear ultrasonic techniques. However, the accumulation of dislocations throughout the continuum (with increasing fatigue) will cause a nonlinear distortion in an ultrasonic wave propagating in the material, and thus generate higher harmonic components in an initially monochromatic ultrasonic wave signal. For this reason, nonlinear ultrasonic (acoustic) waves can be used to quantify the presence and the density of dislocations in a metallic material, and thus measure fatigue damage in a quantitative fashion. In addition, nonlinear ultrasonics has the potential to promote an understanding of the evolution and accumulation of the dislocation substructures in the very early stages of fatigue.

To date, a number of investigators[1–8] have applied nonlinear ultrasonic techniques to assess fatigue damage in different materials under relatively controlled laboratory conditions. Yost and Cantrell[1] and Cantrell and Yost[6] experimentally observed changes of the acoustic nonlinearity parameter, and attributed the changes to the effects of fatigue-induced dislocations. Frouin *et al.*[5,8] performed *in situ* nonlinear ultrasonic measurements during fatigue testing, and related the measured increase in the acoustic nonlinearity parameter—in the vicinity of the fracture surface—to an increase in the dislocation density. Among these studies, only Frouin *et al.*[8] reported using nonlinear ultrasonic results to track fatigue damage throughout the entire fatigue life of a specimen. One field application of nonlinear ultrasonics examined fatigue damage in stainless-steel turbine blades.[7] In spite of the recognized potential of nonlinear ultrasonics, there are very few examples of its successful application to monitor fatigue damage. This is probably due to instrumentation issues that make accurate and consistent nonlinear ultrasonic measurements difficult, plus a lack of flexibility in the measurement setup needed to interrogate real fatigue test specimens. A critical next step—for the incorporation of nonlinear ultrasonic techniques into life-prediction strategies of structural components—is a system-

[a]Also at: School of Civil and Environmental Engineering, Georgia Institute of Technology, Atlanta, GA 30332-0355; electronic mail: laurence.jacobs@ce.gatech.edu

atic study that quantifies the robustness, accuracy, and validity of nonlinear ultrasonics to detect the early stages of fatigue damage (prior to crack initiation) in metallic materials. Of particular interest is the development of an experimental procedure with the capability of performing field inspections of an absolute and repeatable nature.

The objective of the current research is to develop a robust experimental procedure to track the evolution of fatigue damage in metallic materials with the acoustic nonlinearity parameter, β. The effectiveness of this proposed measurement procedure is demonstrated by making repeatable acoustic measurements of β, in nickel-base superalloy specimens, subjected to three types of damage: Quasi-static monotonic, low-, and high-cycle fatigue. These nonlinear ultrasonic measurements are used to track the evolution of damage in multiple specimens with a series of interrupted mechanical tests—first by making a baseline measurement of β in an undamaged specimen, then introducing some damage into the specimen, repeating the measurement of β in this same (unloaded) specimen, then introducing more damage into the specimen, and repeating the procedure.

It is important to note that the acoustic nonlinearity parameter, β, is an absolute material constant, which can be related to the higher-order elastic constants, of a material; the β parameter is a directly measurable acoustic parameter that is linked to the state of material damage. As a result, nonlinear ultrasonics is unparalleled in its potential to provide a robust and quantitative characterization of fatigue damage in in-service structural components. However, the acoustic nonlinearity associated with fatigue damage is very small, and can be easily overwhelmed by a number of other factors (especially instrumentation nonlinearity) inherent to the measurement procedure. Therefore, a critical contribution of this research is a systematic experimental procedure that can identify and remove spurious sources of nonlinearity, isolating only those contributions due to the material and associated damage.

II. GENERATION OF HIGHER HARMONICS AND THE ACOUSTIC NONLINEARITY PARAMETER, β

The equations of motion of a solid element, in the absence of body forces, are written in material coordinates, $\boldsymbol{X}$, as

$$\rho\frac{\partial^2 u_i}{\partial t^2}=\frac{\partial \sigma_{ij}}{\partial X_j}, \tag{1}$$

where t is time, ρ is the mass density, u_i is the displacement vector, and σ_{ij} is the stress tensor. The stress in a nonlinear (fatigued) solid can, in general, be written as

$$\sigma_{ij}=\sigma_{ij}^0+A_{ijkl}\frac{\partial u_k}{\partial X_l}+\frac{1}{2}A_{ijklmn}\frac{\partial u_k}{\partial X_l}\frac{\partial u_m}{\partial X_n}+\cdots, \tag{2}$$

where σ_{ij}^0 is the residual stress in the material, and A_{ijkl} and A_{ijklmn} are the Huang coefficients,[9] which are related to the second- and third-order elastic constants by $A_{ijkl}=\sigma_{jl}^0\delta_{ik}+\bar{C}_{ijkl}$ and $A_{ijklmn}=\bar{C}_{ijklmn}+\bar{C}_{jlmn}\delta_{ik}+\bar{C}_{ijnl}\delta_{km}+\bar{C}_{jnkl}\delta_{im}$. $\bar{C}_{ijkl}$ and $\bar{C}_{ijklmn}$ are modified by fatigue damage (dislocation substructures)[9] from their initial values, C_{ijkl} and C_{ijklmn}.[11] Expressions for the modified elastic constants during fatigue have been presented in terms of the residual stress and plastic strain.[12] The density of a material undergoing finite deformation is given by $\rho=\rho_0/\det\mathbf{F}$ where ρ_0 is the constant density in the unstressed configuration and $\mathbf{F}$ is the deformation gradient tensor, defined as $F_{ij}=\delta_{ij}+\partial u_j/\partial X_i$. Substituting Eq. (2) into Eq. (1), and considering one-dimensional wave propagation of a longitudinal wave in an isotropic solid, one gets

$$\frac{\partial^2 u_1}{\partial t^2}=c^2\frac{\partial^2 u_1}{\partial X_1^2}\left(1+\beta\frac{\partial u_1}{\partial X_1}\right), \tag{3}$$

where $c=\sqrt{(\bar{C}_{1111}+\sigma_{11}^0)/\rho}$ is the longitudinal wave speed and β is the acoustic nonlinearity parameter defined as

$$\beta=\frac{\bar{C}_{111111}+3\bar{C}_{1111}}{\bar{C}_{1111}+\sigma_{11}^0}. \tag{4}$$

It is well known that the second-order elastic constant [$\bar{C}_{1111}$ in Eq. (4)] changes very little, and that the residual stress (σ_{11}^0) is relatively small compared to the elastic constants. Therefore, it is the third-order elastic constant [$\bar{C}_{111111}$ in Eq. (4)] which causes the increase in the acoustic nonlinearity parameter, β, during fatigue.

Consider a time-harmonic plane (displacement) wave $A_1\cos(kX_1-\omega t)$, where A_1 is the amplitude, k is the wave number, and ω is the angular frequency. Assuming that the nonlinearity in the solid is small, the solution to Eq. (3) for this time-harmonic wave is obtained by a perturbation analysis as[13]

$$\begin{aligned}u_1&=-\tfrac{1}{8}\beta k^2A_1^2X_1+A_1\cos(kX_1-\omega t)\\&\quad+\tfrac{1}{8}\beta k^2A_1^2X_1\cos[2(kX_1-\omega t)]+\cdots\\&=A_0+A_1\cos(kX_1-\omega t)+A_2\cos[2(kX_1-\omega t)]+\cdots.\end{aligned} \tag{5}$$

It is noted that the amplitude of the second-harmonic displacement is proportional to the acoustic nonlinearity parameter and a subharmonic; that is, the static displacement is induced by the material nonlinearity.[14] The acoustic nonlinearity parameter is determined experimentally by measuring the absolute amplitudes of the fundamental (A_1) and the second-harmonic (A_2) displacement signals, or

$$\beta=\frac{8A_2}{k^2X_1A_1^2}. \tag{6}$$

Finally, note that Eq. (6) neglects the effect of attenuation losses that may be present in the fundamental and second-harmonic. If the difference in attenuation rates at the fundamental and the second-harmonic frequencies is large, then a correction factor must be included in the measurement of β. The specific superalloy examined in this research is IN100, which is produced by powder metallurgy and has a very fine grain structure. Attenuation measurements are made in IN100 through the range of 1–15 MHz before fatigue tests. These results show that the attenuations at the fundamental and the second-harmonic frequencies are about

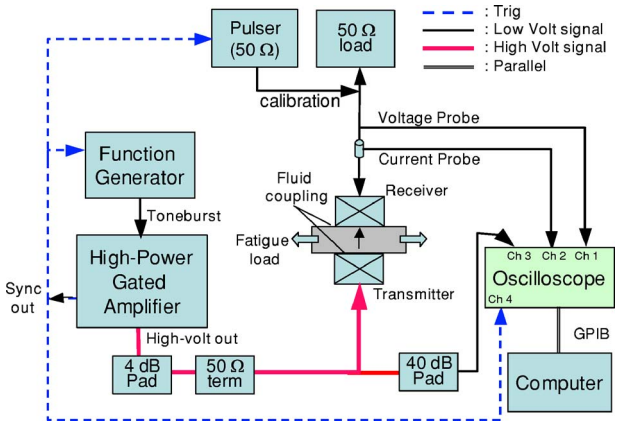

FIG. 1. (Color online) Experimental setup.

0.14 Neper/cm and 0.34 Neper/cm, respectively, which correspond to a maximum correction of less than 2% in β. Furthermore, the fatigue specimens show no noticeable change in attenuation in the frequency range considered here, so no attenuation corrections are made for the following β calculations.

III. EXPERIMENTAL PROCEDURE

A. Measurement system and procedure

Figure 1 shows a schematic of the proposed nonlinear ultrasonic measurement system. A tone burst signal of 7–9 cycles (depending on the specimen thickness) at 5.3 MHz is generated by a function generator (80 MHz Agilent 33250A) and is fed into a high-power gated amplifier (Ritec RAM-10000). In order to ensure one-dimensional wave propagation in a single direction (only right or left propagating), the exact number of cycles of the tone burst is selected as the maximum number of cycles that can fit within the thickness of the specimen—the spatial length of the tone burst is less than the specimen thickness. This eliminates any possible spurious (apparent) higher harmonics generated by the interference of the incident and reflected wavefronts, as well as the effects of boundary conditions. The amplified high-voltage signal passes through a 4 dB attenuator (pad) and a 50 Ω termination to suppress the transient behavior due to the mismatch in electrical impedances between the amplifier and the transducer. Commercial narrow-band PZT (Lead Zirconate Titanate)-base piezoelectric transducers, with center frequencies of 5 MHz and 10 MHz, are used as a transmitter and a receiver, respectively. The transducers are coupled to the specimen with light lubrication oil. A special fixture is designed to keep both the transmitting and receiving transducers aligned on the same centerline axis, and to also allow for the removal of either transducer (transmitter or receiver) without disturbing the coupling (and position) of the other; this capacity is critical for the calibration procedure described next. The receiver is terminated with a 50 Ω passive load to have the same terminal load in the calibration. Both voltage and current signals of the transmitted ultrasonic waves are recorded and averaged 256 times with an oscilloscope, and then transferred to a computer for further signal processing. Then, diffraction corrections are made to the measured fundamental and the second-harmonic signal amplitudes.

The calibration procedure for the (piezoelectric) receiving transducer is based on the principle of self-reciprocity,[15] and is employed in order to obtain a conversion transfer function (from the measured electrical signal to the absolute amplitude of the particle displacement), and to compensate for any (small) variations in the coupling of the receiving transducer. Note that this calibration is performed prior to every nonlinear measurement, with the transmitter transducer removed. A 50 MHz pulser/receiver (Panametrics, 5072PR) is used to transmit (through the receiver transducer) a wide-band ultrasonic pulse through the specimen. The current and voltage signals of the incident and the reflected pulse from the bottom surface of the specimen that is kept stress-free (when the transmitter is removed), are measured and used to calculate a transfer function that converts the measured current signal to the particle displacement of the incident wave at the receiver.[15]

Finally, the pulse-inversion technique[16,17] is applied to accentuate the contribution of the even (second) harmonic signal, while reducing the dominance of the fundamental contribution. The pulse-inversion technique is very efficient in extracting this second-harmonic amplitude by canceling out the odd harmonics (which are mainly due to the instrumentation); the even harmonic signal is extracted by adding two 180° out-of-phase input signals.[18] Figure 2 illustrates the pulse-inversion technique by showing both the 0° phase, and the 180° out-of-phase (inverted) signals, the respective Fourier spectra before and after addition (in the time domain), and the second-harmonic signal extracted. For the actual procedure, first, two transmitted time domain signals with 180° out-of-phase inputs are measured consecutively with all other conditions unchanged. A function generator performs phase inversion of the input pulse. Then, two separately measured output signals are combined in the time domain, extracting the second-harmonic signal. Note that this combination is performed with two raw signals without introducing any adjustments, such as time shifts or amplitude modification. Figure 2 clearly demonstrates how the fundamental frequency contribution is completely canceled out, leaving only the second-harmonic contribution. Note that the remaining subharmonic component (at zero frequency) corresponds to the first term in Eq. (5), and appears as a result of the static displacement induced by the acoustic radiation; this component should have an amplitude proportional to the amplitude of the second-harmonic,[19] but it is not systematically analyzed in this study. The frequency spectra of the signal originally transmitted, and the extracted signal shown in Fig. 2(b) are independently calculated with a rectangular window. Finally, to obtain a more accurate estimation of the amplitudes of the fundamental and second-harmonics, the signals are digitally filtered in the frequency domain and inverse Fourier transformed. An additional advantage of using the pulse-inversion technique is that one can readily monitor the shape of the second-harmonic signal. Since the amplitude of the second-harmonic signal produced by material nonlinearity is very small in comparison to the amplitude of the fundamen-

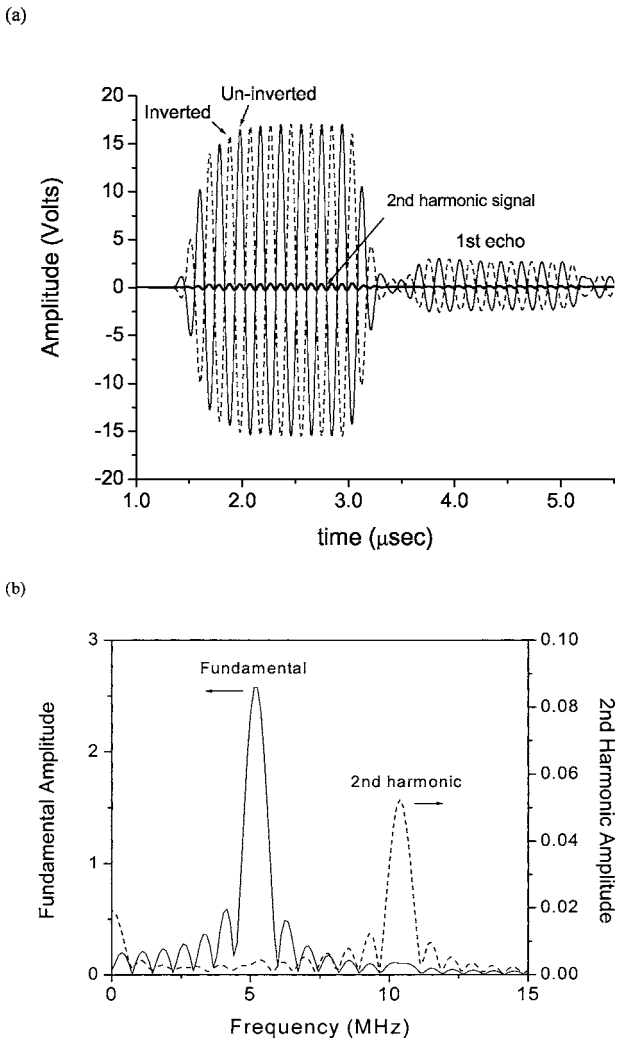

FIG. 2. (a) Typical time domain signals: Thin continuous and dotted lines are the transmitted signals with 0° phase (uninverted) and 180° out-of-phase (inverted) inputs, respectively. The thick line is the second-harmonic signal extracted by the pulse-inversion technique. (b) Fourier spectra of the original transmitted signal (fundamental) and the second-harmonic signal extracted by the pulse-inversion technique, demonstrating that the second-harmonic amplitude can be measured without being influenced by the large fundamental amplitude.

tal, small variations in coupling—that are usually accompanied by spurious interface nonlinearity—can have a significant influence on the repeatability of the proposed measurement procedure. Experience shows that the shape of this second-harmonic signal is an excellent indicator of the quality of the transducer to specimen coupling.

Figure 3 illustrates the linear relationship that exists between the measured absolute amplitudes of the second-harmonic and the squared fundamental (both displacements), as a function of increasing input voltage amplitude. These absolute displacement amplitudes are calculated using the transfer function described previously. Figure 3 shows the results of two independent measurements on the same specimen, where the transducers and the couplant are completely removed, and then reattached and recalibrated for the second measurement. It is seen that the slopes from these two independent measurements are nearly constant, which confirms that the measurements are repeatable, and that removal and

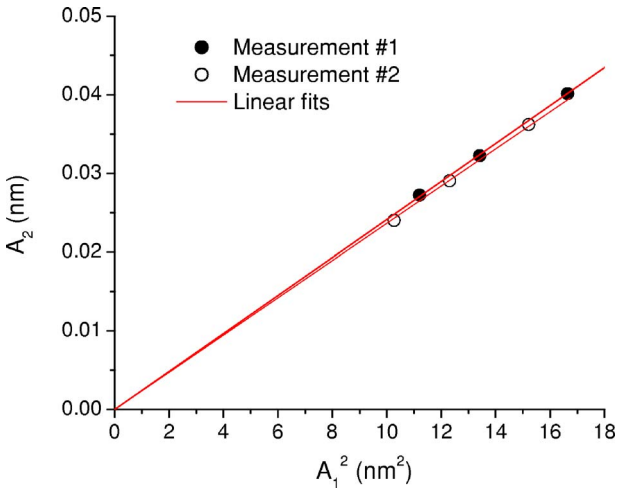

FIG. 3. (Color online) Second-harmonic amplitude (A_2) versus the amplitude of the fundamental squared $[(A_1)^2]$ for increasing input voltage obtained from two independent measurements.

replacement of the transducers (and couplant) will not have a dominant (negative) influence on the results. The variability (error bars) due to measurement error is determined by averaging five measurements on the same undamaged specimen, and results in a variability of ±0.45 on all β values reported henceforth. Finally, Fig. 3 can be used as a guide for the required input voltage needed to avoid inconsistencies caused by a low fundamental amplitude.[20]

The measurement system is calibrated by measuring β in borosilicate. It is known that borosilicate has a very low degree of nonlinearity, and researchers[21] have shown that the ratio of the second-harmonic amplitude to the fundamental amplitude is on the order of −120 dB (this unpublished reference value illustrates that the β of borosilicate is almost zero). A β of 9.0 is measured in borosilicate using the proposed measurement procedure, and this nonzero value of β is believed to be associated with the inherent nonlinearity of the transmitting piezoelectric transducers used in the measurement system. This is in agreement with previous researchers[22] who examined the nonlinear properties of PZT (polarized K1) and measured its β to be on the order of 8.0. Therefore, a β of 9.0 will be used to calibrate the measurement system by subtracting this value from all measured β values. Although such a calibration method neglects the interactions between different frequencies in a nonlinear system, it can be easily argued that the effects of such interactions on β are higher ordered. This is further verified by performing a β measurement on fused silica. The directly measured value of β for fused silica is 21.0. After calibration (subtracting 9.0), a β of 12.0 is obtained for fused silica, which is in agreement with published values.[23]

The good agreement between these results and published values, plus the consistency and repeatability of the results reported in Sec. IV, validate the accuracy of the proposed procedure as a working method to track changes in β as a function of fatigue life in multiple specimens.

B. Specimens

Three different types of specimens are used; each type machined from IN100 cylindrical rods—128 mm long and

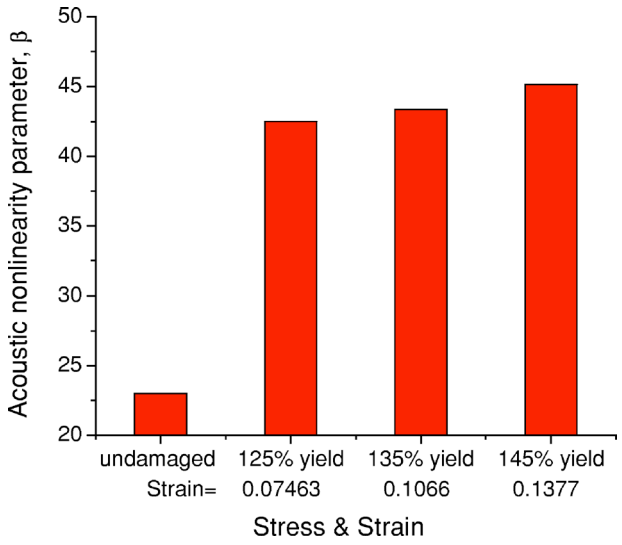

FIG. 4. (Color online) Monotonic load results—acoustic nonlinearity parameter β versus applied stress (or strain) level.

27 mm in diameter. Note that the surface finishes on all specimens in this study are "as-machined." The first type is a standard fatigue specimen with a constant rectangular cross section—a constant gauge width of 12.5 mm and a thickness of 6.4 mm. One of these specimens is used for the low-cycle fatigue tests, and one is used for the high-cycle fatigue tests. The second specimen has an hour-glass shape (starting from a width of 12.5 mm and a constant thickness of 6.4 mm) with a varying cross section that gradually reduces to create a region of higher stress at its center; this specimen is used exclusively for the high-cycle fatigue tests. The third specimen is a nonstandard rectangular bar specimen; it is simply a 120 mm long by 14.3 mm wide rectangular bar—having a constant thickness of 4.7 mm. This specimen is used for both the monotonic and low-cycle fatigue tests, and for a concurrent set of Rayleigh wave measurements.[24]

IV. EXPERIMENTAL RESULTS AND DISCUSSION

A. Monotonic load results

First, consider a quasi-static monotonically loaded (nonstandard rectangular bar) specimen. This specimen is used to validate the repeatability of a set of nonlinear ultrasonic measurements made on a specimen subjected to an interrupted mechanical test—a test specimen that is mechanically loaded, removed to make a set of nonlinear ultrasonic measurements, and then the procedure is repeated at specified intervals, typically until the specimen fails. In this monotonic test, the specimen is loaded (at a rate of 890 N/s) to a first-load equivalent to 125% of the yield stress (absolute strain of 7.463%), and then is unloaded at the same rate. The nonlinear ultrasonic measurements are then performed on the unloaded specimen. The same procedure is repeated for increasing maximum loads equivalent to 135% and 145% of yield stress (strains of 10.66% and 13.77%, respectively). These calibrated results are presented in Fig. 4, and note that these measured acoustic nonlinearity parameters, β, are absolute values. It is important to note that the β value of 23.1—measured in the undamaged specimen (before any mechanical load is applied)—is a measure of the intrinsic nonlinearity of the undamaged IN100 material; and that the nonlinearity associated with the transmitting piezoelectric transducers (β=9.0) has already been subtracted from this and all other values. Figure 4 shows that there is a significant increase in β with increasing plastic stress; the increase is largest from the unloaded (undamaged) state to 125% yield stress, and then the increase is less substantial at the higher stresses. This observed behavior of a large increase in the acoustic nonlinear parameter, once the specimen is loaded above its yield stress, makes sense because dislocations (or microplasticity) create significant material nonlinearity; the literature reports that the second- (order) harmonic amplitudes associated with dislocations should be larger than the intrinsic material nonlinearity due to the elastic lattice anharmonicity.[25] Most importantly, the results in Fig. 4 show that the proposed measurement procedure is capable of making an absolute measurement of the evolution of the acoustic nonlinear parameter, β (as a function of stress in this case) in these interrupted mechanical tests on an IN100 specimen.

B. Low-cycle fatigue results

Low-cycle fatigue in this paper refers to a fatigue test where the maximum stress is above yield, so there is plastic deformation even at the beginning of the fatigue test. Of equal importance is that cyclic loading promotes the formation of dislocation dipoles, which is the strongest source of nonlinearity among a list of potential sources.[6,9,10] The frequency of cyclic loading is 0.5 Hz, $R(=\sigma_{\min}/\sigma_{\max})$ is zero (strain controlled), the maximum stress level is 105% of the yield stress (strain of 0.48%), and the fatigue tests are interrupted to perform the nonlinear ultrasonic measurements at different numbers of fatigue cycles. Three different specimens are tested, and there will be some level of variability associated with the initial microstructure of each specimen. As a result, the measured acoustic nonlinearity parameters will be normalized by the value measured in each undamaged specimen (β_0), before any mechanical load is applied. This normalization procedure (which will be repeated for the high-cycle fatigue results) removes some of the variability associated with the initial microstructures of each specimen, enables a direct comparison of the evolution of the acoustic nonlinearity of all the specimens tested, and normalizes the nonlinearity associated with the transmitting piezoelectric transducers. The evolution of the normalized acoustic nonlinearity parameter (β/β_0), as a function of normalized fatigue life (fatigue cycle normalized to the total number of cycles, where 100% means the total fatigue life), together with a best-fit curve, is shown in Fig. 5. Note that the specimens failed at 12,640, 13,012, and 50,221 cycles (the third specimen is the standard fatigue specimen; while the first two are the nonstandard rectangular bars) and the (calibrated) β_0 measured in each specimen is 21.4, 22.2, and 22.4, respectively.

Figure 5 shows a rapid increase in β/β_0 (up to 30%) during the first 40% of fatigue life, which demonstrates that these nonlinear ultrasonic measurements can be used to quantitatively characterize the damage state of this material

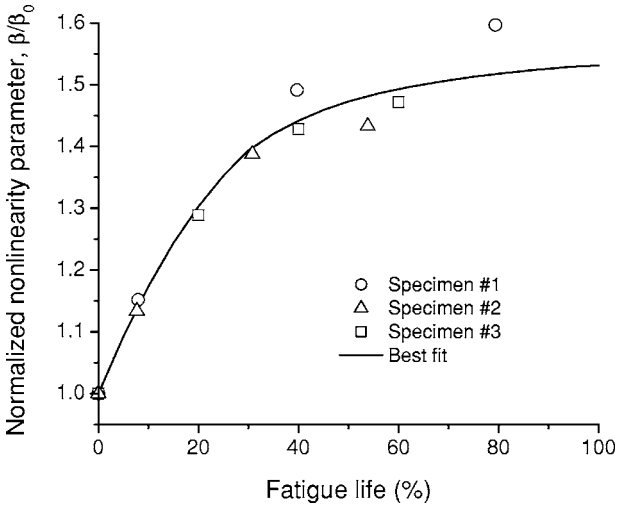

FIG. 5. Low-cycle fatigue results—normalized acoustic nonlinearity parameter β/β_0 as a function of the percentage of fatigue life for three different fatigue specimens. The continuous line is the best-fit curve obtained from the discrete experimental data.

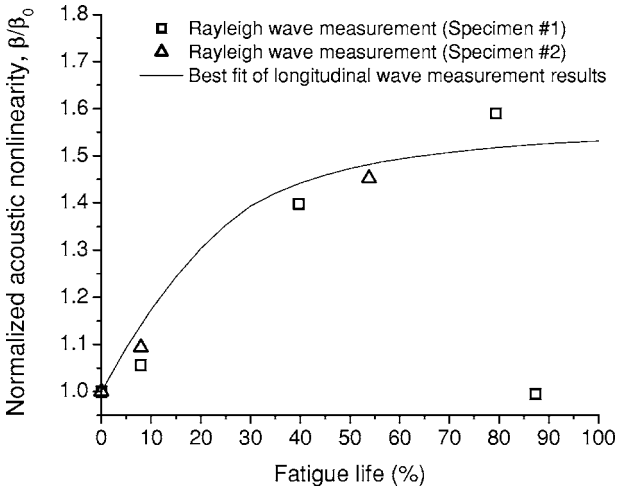

FIG. 6. Comparison of longitudinal and Rayleigh wave (Ref. 24) results showing the normalized acoustic nonlinearity parameter β/β_0 as a function of the percentage of fatigue life for the low-cycle fatigue results.

in the early stages of fatigue life. This is somewhat different from other experimental results,[5] which show a slower initial increase in β. The difference in behavior is most likely due to the high maximum stress (strain) level beyond the yield stress (strain), and a significant amount of plasticity—due to the dislocation motions—probably starts accumulating in the specimen from the first loading cycle, which reduces the time period for dislocation reassociation at the beginning of fatigue. The measurement data show increasing scatter with increasing number fatigue cycles, which is most likely due to a combination of two factors: The intrinsic material behavior, and issues with the measurement procedure. There is an inherent randomness in the progression of fatigue damage during fatigue testing (more so in high-cycle fatigue, as discussed in the next section), which should manifest itself as a corresponding randomness in the resulting acoustic nonlinearity. There is a somewhat unrelated issue with the measurement procedure in the later stages of fatigue—the surface deformation associated with the increased plasticity makes it difficult to consistently couple the transducers to the specimen surface. Finally, note that a best-fit curve, such as the one developed in Fig. 5 (but based on a larger number of specimen and data points), has the potential to serve as a master curve for life prediction based on nonlinear ultrasonic measurements.

A companion study makes nonlinear ultrasonic measurements with Rayleigh surface waves on the first two specimens; the procedure used to make these (relative) nonlinear Rayleigh wave measurements is reported elsewhere.[24] Figure 6 shows a comparison of the best-fit curve from Fig. 5 (longitudinal waves) with those from the nonlinear Rayleigh wave measurements. There is excellent agreement with these two sets of results, demonstrating that both longitudinal and Rayleigh waves can be used to track nonlinear material behavior. Note that the sharp drop in the acoustic nonlinearity (the single data point in Fig. 6), at 87% of fatigue life for Specimen No. 1, is most likely due to the emergence of surface-breaking microcracks whose depths are larger than the wavelength of the second-harmonic.[24]

C. High-cycle fatigue results

High-cycle fatigue in this study refers to fatigue tests where the maximum stress level is below yield; in this case, the maximum stress is 95% of yield stress, the frequency of cyclic loading is 1 Hz, and R $(=\sigma_{\min}/\sigma_{\max})$ is zero (load controlled). Five different fatigue specimens are tested, with failure occurring at 55,432, 102,392, 203,220, 328,341, and 350,985 cycles. As with the monotonic and low-cycle fatigue tests, these fatigue tests are interrupted to perform the nonlinear ultrasonic tests. Figure 7 shows the change in the normalized acoustic nonlinearity parameter (β/β_0) over the normalized fatigue life of each specimen. Note that the (calibrated) β_0 measured in each specimen is 22.1, 21.3, 19.8, 22.4, and 21.2, respectively.

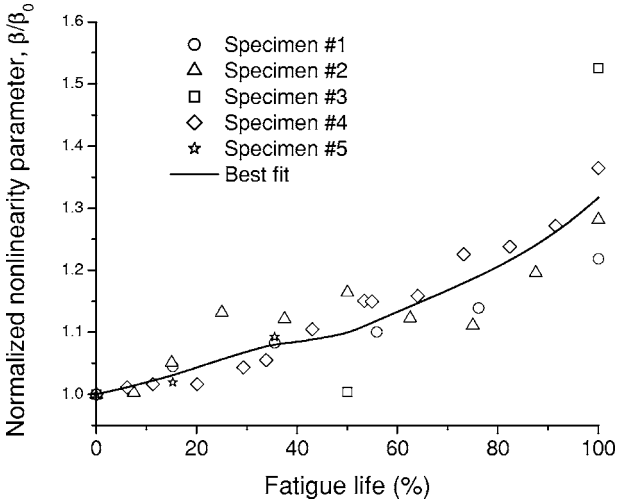

FIG. 7. High-cycle fatigue results—normalized acoustic nonlinearity parameter β/β_0 as a function of the percentage of fatigue life for five different fatigue specimens. The continuous line is the best-fit curve obtained from the discrete experimental data.

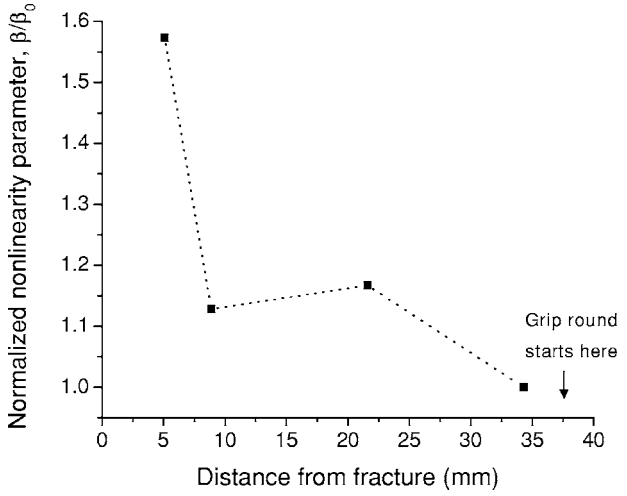

FIG. 8. Spatial variation of the normalized acoustic nonlinearity parameter on one failed high-cycle fatigue specimen, shown as a function of distance from the fracture site.

The critical observations from Fig. 7 are: The absolute increase in acoustic nonlinearity is much lower than that of the low-cycle fatigue tests; there is much more scatter in the high-cycle fatigue data (a larger variability at a given percentage of fatigue life than the data from the low-cycle fatigue tests); and the overall increase in acoustic nonlinearity is more gradual in the high-cycle specimens. Some of these trends may be inherent to the high-cycle fatigue behavior of this material since fatigue damage during high-cycle fatigue is more localized than that during low-cycle fatigue. So it is not surprising that there is a corresponding variability in the acoustic nonlinearity. Similar results were obtained in a titanium alloy (Ti-6-4) by Frouin *et al.*[8] A full explanation of this behavior may only be possible by coupling these nonlinear ultrasonic results with a material model that predicts the formation of dislocation substructures in this material under different loading conditions. For Specimen No. 5, additional nonlinear measurements beyond 35% of fatigue life were not possible due to severe surface distortion, but the fatigue test was continued to obtain its fatigue life (55,432).

Nonlinear ultrasonic evidence of this localized damage behavior in high-cycle fatigue is given in Fig. 8 by plotting the spatial variation (four discrete locations) of the acoustic nonlinearity in the gauge section of a failed high-cycle fatigue specimen (the specimen with a uniform cross section). Note that each acoustic nonlinearity parameter measured with this experimental procedure is representative of the cylindrical volume of material under the transducer (12.7 mm diameter for these tests). Figure 8 shows that the acoustic nonlinearity, at a location about 5 mm away from the fracture surface, is approximately 58% higher than those in the region near the grip. It is also shown that the fatigue damage in this material is quite localized (on the order of 10 mm), which could be the source of the large variation in the later stages of the high-cycle fatigue tests. It is important to note that this level of spatial variation in the acoustic nonlinearity parameter (and thus, localized damage) is primarily present in the high-cycle fatigue specimens; and for these specimens, mainly in the later stages of fatigue life. The monotonic and low-cycle fatigue specimens do not show this level of spatial variation in the measured acoustic nonlinearity parameter. These values are very consistent, regardless of where they are measured in the gauge section, so the damage in the monotonic and low-cycle fatigue specimens seems to be more evenly distributed.

V. CONCLUSION

This research develops a robust experimental procedure to track the evolution of fatigue damage in a nickel-base superalloy with the acoustic nonlinearity parameter, β, and demonstrates its effectiveness by making repeatable measurements of β on multiple specimens subjected to both high- and low-cycle fatigue. The measurement procedure developed in this research is robust in that it is based on conventional piezoelectric contact transducers—which are readily available off the shelf—and offers the potential to be used in field applications. In addition, it allows the user to isolate sample nonlinearity from measurement system nonlinearity. The experimental results show that there is a significant increase in β associated with the high plasticity of low-cycle fatigue, and illustrate how these nonlinear ultrasonic measurements quantitatively characterize the damage state of a specimen in the early stages of fatigue. A companion study with Rayleigh surface waves demonstrates that both longitudinal and Rayleigh waves can be used to track nonlinear material behavior. The high-cycle fatigue results are less definitive (the increase in β is not as substantial), but still show a clear relationship between β and remaining fatigue life. Overall, these nonlinear ultrasonic results indicate that the fatigue damage associated with high-cycle fatigue is relatively localized, while the damage associated with low-cycle fatigue is more evenly distributed. One application of the measured β versus fatigue life data is to potentially serve as a master curve for life prediction based on nonlinear ultrasonic measurements.

ACKNOWLEDGMENTS

This material is based upon work supported by the Defense Advanced Research Projects Agency (DARPA), Defense Sciences Office (DSO), Engine Systems Prognosis—under a subcontract to Prime Contract No. HR0011-04-C-0001, and is approved for public release with unlimited distribution. The authors thank Jeff Davies, Jan Herrmann, and Marc Erwin, for their help with the measurements, and Professor Peter Nagy for his advice and the use of his Ritec RAM-10000 system.

[1]W. T. Yost and J. H. Cantrell, "The effects of fatigue on acoustic nonlinearity in aluminum alloys," Proc. IEEE **2**, 947–954 (1992).
[2]J. K. Na, J. H. Cantrell, and W. T. Yost, "Linear and nonlinear properties of fatigued 410Cb stainless steel," Rev. Prog. Quant. Nondestr. Eval. **15**, 1479–1488 (1996).
[3]D. J. Barnard, G. E. Dace, and O. Buck, "Acoustic harmonic generation due to thermal embrittlement of Inconel 718," J. Nondestruct. Eval. **16**, 67–75 (1997).
[4]P. B. Nagy, "Fatigue damage assessment by nonlinear ultrasonic material characterization," Ultrasonics **36**, 375–381 (1998).
[5]J. Frouin, S. Sathish, T. E. Matikas, and J. K. Na, "Ultrasonic linear and nonlinear behavior of fatigued Ti-6Al-4V," J. Mater. Res. **14**, 1295–1298 (1999).

[6]J. H. Cantrell and W. T. Yost, "Nonlinear ultrasonic characterization of fatigue microstructures," Int. J. Fatigue **23**, S487–S490 (2001).
[7]Y. L. Hinton, J. K. Na, W. T. Yost, and G. L. Kissel, "Field measurement of the acoustic nonlinearity parameter in turbine blades," NASA Technical Memorandum, TM-2000-210303 ⟨http://library-dspace.larc.nasa.gov/dspace/jsp/bitstream/ 2002/13099/1⟩ (2000).
[8]J. Frouin, T. E. Matikas, J. K. Na, and S. Sathish, "*In situ* monitoring of acoustic linear and nonlinear behavior of titanium alloys during cyclic loading," Proc. SPIE **3585**, 107–116 (1999).
[9]J. H. Cantrell, "Substructural organization, dislocation plasticity, and harmonic generation in cyclically stressed wavy slip metals," Proc. R. Soc. London, Ser. A **460**, 757–780 (2004).
[10]J. H. Cantrell, "Quantitative assessment of fatigue damage accumulation in wavy slip metals from acoustic harmonic generation," Philos. Mag. **86**, 1539–1554 (2006).
[11]M. A. Breazeale and J. Philip, "Determination of third-order elastic constants from ultrasonic harmonic generation measurements," Phys. Acoust. **17**, 1–60 (1984).
[12]J.-Y. Kim, J. Qu, L. J. Jacobs, J. Littles, and M. F. Savage, "Acoustic nonlinearity parameters due to microplasticity," J. Nondestruct. Eval. **25** (2006).
[13]R. E. Green, Jr., "Ultrasonic investigation of mechanical properties," *Treatise on Materials Science and Technology* (Academic, New York, 1973), Vol. **3**.
[14]J. H. Cantrell, Jr., "Acoustic-radiation stress in solids. I. Theory," Phys. Rev. B **30**, 3214–3220 (1984).
[15]G. E. Dace, R. B. Thompson, and O. Buck, "Measurement of the acoustic harmonic generation for materials characterization using contact transducers," Rev. Prog. Quant. Nondestr. Eval. **11**, 2069–2076 (1992).
[16]Y. Ohara, K. Kawashima, R. Yamada, and H. Horio, "Evaluation of amorphous diffusion bonding by nonlinear ultrasonic method," Rev. Prog. Quant. Nondestr. Eval. **23**, 944–951 (2004).
[17]S. Krishnan, J. D. Hamilton, and M. O'Donnell, "Suppression of propagating second harmonic in ultrasound contrast imaging," IEEE Trans. Ultrason. Ferroelectr. Freq. Control **45**, 704–711 (1998).
[18]T. Mueller, "Characterization of microstructure evolution of nickel-base superalloys using nonlinear ultrasonic techniques." M.S. thesis, School of Civil and Environmental Engineering, Georgia Institute of Technology, 2005.
[19]W. T. Yost and J. H. Cantrell, Jr., "Acoustic-radiation stress in solids. II: Experiment," Phys. Rev. B **30**, 3221–3227 (1984).
[20]D. J. Barnard, "Variation of nonlinearity parameter at low fundamental amplitudes," Appl. Phys. Lett. **74**, 2447–2449 (1999).
[21]B. B. Chick and M. McKenna (RITEC Corporation, private communication, 2005).
[22]K. K. Na and M. A. Breazeale, "Ultrasonic nonlinear properties of lead zicronate-titanate ceramics," J. Acoust. Soc. Am. **95**, 3213–3221 (1994).
[23]D. C. Hurley and C. M. Fortunko, "Determination of the nonlinear ultrasonic parameter β using a Michelson interferometer," Meas. Sci. Technol. **8**, 634–642 (1997).
[24]J. Herrmann, J.-Y. Kim, L. J. Jacobs, J. Qu, J. W. Littles, and M. F. Savage, "Assessment of material damage in a nickel-base superalloy using nonlinear Rayleigh surface waves," J. Appl. Phys. **99**, 124913 (2006).
[25]A. Hikata and C. Elbaum, "Generation of ultrasonic second and third harmonics due to dislocations," Phys. Rev. **144**, 469–477 (1966).